Cylindrical transparent conductive oxide-free dye-sensitized solar cells with treated flat titanium sheet

Azwar Hayat[a,*] **Ajay Kumar Baranwal**[b] **Masaki Nakamura**[c] **Fujisawa Shigeki**[c] **Shyam S. Pandey**[d] **and Shuzi Hayase**[b,*]

[a]Hasanuddin University, Department of Mechanical Engineering, Faculty of Engineering, Gowa, Indonesia

[b]The University of Electro-Communications, i-Powered Energy System Research Center (i-PERC), Tokyo, Japan

[c]Ushio Inc., Tokyo, Japan

[d]Kyushu Institute of Technology, Graduate School of Life Science and Systems Engineering, Fukuoka, Japan

Abstract. Conventional dye-sensitized solar cells (DSSCs) require two transparent conductive oxide (TCO) glasses as working and counter electrodes and are one of the most costly components posing an appreciable cost burden for production and commercialization. To circumvent this issue, we propose a TCO-free device structure utilizing titanium (Ti) sheets as a substitute for TCO. This back contact device structure not only allows the removal of the costly TCO component from the working electrode but also enhances the extent of photons absorbed by the photoanode. A flat titanium sheet with microholes (FTS-MH) was successfully applied to fabricate cylindrical TCO-free-DSSCs) with a titanium sheet as a back contact electrode. When the H_2O_2 surface-treated FTS-MH substrate generating dense anatase TiO_2 nanosheets was used as a photoanode, there was a pronounced improvement in efficiency from 5.76% to 8.59%. This was mainly attributed to the lower interfacial resistance facilitated by improved electrical contact between the conducting FTS-MH substrate and mesoporous TiO_2 layer since enhancement in the dye loading was only 8.6%. © *2022 Society of Photo-Optical Instrumentation Engineers (SPIE)* [DOI: 10.1117/1.JPE.12.045502]

Keywords: cylindrical; dye-sensitized solar cell; transparent conducting oxide free; back contact.

Paper 22023G received Apr. 9, 2022; accepted for publication Nov. 15, 2022; published online Dec. 2, 2022.

1 Introduction

State-of-art dye-sensitized solar cells (DSSCs) with photoconversion efficiency surpassing amorphous silicon solar cells have attracted immense attention owing to relatively lower cost of production, colorful, transparency, and very good performance, especially under low-light intensities.[1] Typically, DSSC consists of working and counter electrodes utilizing transparent conducting oxide (TCO) glasses sandwiching a redox electrolyte. The working electrode consists of dye-adsorbed wide band gap semiconductors such as titanium dioxide (TiO_2), tin dioxide (SnO_2), zinc oxide (ZnO), etc. coated on fluorine-doped tin-oxide (FTO) glass.[2–8] On the other hand, counter electrodes are composed of a thin catalytic layer of carbon, graphene, or platinum coated on the FTO.[9–11] An electrolyte consisting of iodide/triiodide, Co(II)/Co(III), etc. redox couple is filled between the working and counter electrodes to sustain dye-regeneration and complete the DSSC working cycle.[12,13] Nowadays, research on DSSCs is not limited to developing efficient materials for the different components of DSSCs but also moving towards the proposal of novel device structures, which are efficient and cost-effective as compared to conventional solar cells. Removal of the costly TCO components of the conventional DSSCs to reduce the production cost of DSSCs has been attempted by several research groups including

*Address all correspondence to Azwar Hayat, azwar.hayat@unhas.ac.id; Shuzi Hayase, hayase@uec.ac.jp

us in the past. A new solar cell architecture may employ cylindrical solar cells to harvest the photons from all directions, which can be made of thin-film semiconductor material that is deposited on a glass tube. Efforts in this direction had already been made by Solyndra utilizing CIGS solar cells in cylindrical device architecture.[14] However, in September 2011 the company filed for bankruptcy due to the decline in silicon price, which made them unable to compete with conventional crystalline silicon solar cells.[15,16]

Dye-sensitized solar cells (DSSCs) have a low-cost fabrication process compared with silicon-based solar cells.[17] As compared to flat DSSCs, the cylindrical structure has several advantages. Cylindrical solar panels absorb more light in a day, because the sun may fall upon some part of the front curvature exposure of the solar cells during the daytime to produce more power. Besides generating more electricity, cylindrical solar panels offer less wind resistance. The space between the adjacent cylindrical solar cell tubes allows wind to pass through. These kinds of solar cells do not need to be secured or reinforced like conventional solar panels. On the other hand, conventional flat solar panels need to be installed in sun facing direction.[18] Tachan and his group[19] reported the effectiveness of cylindrical architecture wherein the sealing areas can be reduced up to one-third as compared to similar flat solar cells. Our group has been also working in TCO-less DSSCs for the past 7 years.[20,21] Learning from the TCO-less structure, we fabricated a cylindrical TCO-less DSSCs with steel use stainless (SUS) mesh as a photoanode supporter which produced 11.94 mA/cm^2 short circuit current density (Jsc) with 5.58% of photoconversion efficiency (PCE) under AM 1.5 simulated solar irradiation.[22] Nevertheless, SUS mesh required its protection with sputtering Ti over it to retard the back electron transfer. Without the Ti protection, electron recombination was much higher leading to poor PCE.[23,24] Our group also reported coil-type cylindrical DSSCs (CC-DSSCs) with titanium wire to substitute SUS mesh.[25] Titanium wire is strong, lightweight, and does not react with electrolytes, which makes it a better choice than other metals.[26] However, a homogeneous of TiO_2 layer on the top of the wrapped coil in CC-DSSCs is cumbersome and the gap between wires made uneven surface between coil wires TiO_2 layers easy to crack.

The novelty of the present work lies in the utilization of a flat titanium sheet with microholes (FTS-MH) as a photoanode supporter to replace the SUS mesh and titanium wire of CC-DSSCs reported by us previously. FTS-MH allows not only a homogenous and crack-free coating of the TiO_2 layer but also the facile transport of redox species between the working and counter electrodes. Another beauty of our device structure is the use of TiO_2 with a bigger particle size (400 nm) for the initial filling of the microhole and support of the mesoporous TiO_2 layer. This large particle size improves the scattering of the incident light and the Ti-sheet of the counter electrode further reflects the incident light improving overall light trapping in our newly proposed TCO-free cylindrical DSSCs. FTS-MH (20 μm) is a flexible and strong material that is durable enough to bend 360 deg without damaging the performance of photoanodes. Novel TCO-free cylindrical DSSCs employ Ti sheet as a counter electrode and FTS-MH as a photoanode grid making it a robust structure for mass production. FTS-MH allows a facile fabrication of TCO-free cylinder solar cells with ease and simplicity, compared to cylindrical DSSCs reported before.

2 Experimental Detail

2.1 *Materials*

A flat titanium sheet with microholes (FTS-MH) was received from Ushio Inc., Japan. In this experiment, untreated FTS-MH and one treated with H_2O_2 were used as photo-electrodes. Titanium dioxide (TiO_2) PST-400C with 400 nm particle size and PST-30NRD with 30 nm particle size were purchased from Catalysts and Chemical Co. Ltd., Japan. The 0.3 mM solution of Ruthenizer 535-bis TBA [Di-tetrabutylammoniumcis-bis (isothiocyanato) bis (2,2′-bipyridyl-4,4′-dicarboxylato) ruthenium (II)] (N-719) was purchased from OPV Tech (China). Materials used for electrolyte were iodine (I_2), lithium iodide (LiI), 4-tert-butylpyridine, 1,2-dimethyl-3 propylimidazolium iodine, and acetonitrile as solvent. Glass paper with 50-μm thickness as a spacer between photoanode and counter electrode was used. Fluoropolymer Heat Shrink Tube (Junflon NF NF070, FEP) was purchased from JUNFLON Junkosha Inc., Japan.

2.2 *Cell Fabrication*

Cylindrical glass tube with a diameter of 5 mm was wrapped with 80 nm thick platinum (Pt)-sputtered titanium foils having a thickness of 20 μm. Pt catalytic layer was deposited onto Ti foil using a high-rate sputtering apparatus (ULVAC SH-250, room temperature, 200 W, 30 min) at a working pressure of 6.6×10^{-1} Pa. The titanium foil used as a counter electrode has the same properties as the titanium sheet used at the anode. The difference was the microholes are patterned by a chemical etching process by Ushio Inc. To stick them together, a plastic spacer was used as glue. Titanium foil/plastic spacer/cylinder glass was heated at 120°C on a hotplate to melt the spacer while applying pressure on the sandwich structure [Fig. 1(a)]. Photo-electrodes for cylinder TCO-free DSSCs were prepared differently from conventional DSSCs. As a replacement for FTO glass, we used FTS-MH with 20 μm thickness as a photo-anode supporter. FTS-MH was cleaned with an ultrasonic cleaner in acetone for 15 min. After drying with a blower, untreated FTS-MH was coated with TiO_2. For treated FTS-MH, hydrogen peroxide (H_2O_2) treatment was applied to it. H_2O_2 30% (w/w) in H_2O was directly used. The solution was put in a beaker along with FTS-MH and heated at 95°C for 30 min. After treatment, FTS-MH was rinsed with ethanol and dried with a blower. To finish the treatment, calcination at 450°C for 30 min was applied. After cooling down to room temperature, TiO_2 paste with a larger particle size (PST-400C paste) was screen printed onto both treated and untreated FTS-MH using a metal mask (thickness: 40 μm) while putting polytetrafluoroethylene (PTFE) mesh above the FTS-MH to hold the TiO_2. FTS-MH was dried at 125°C for 6 min and PTFE was removed after cooling down to room temperature and baked again at 450°C for 30 min. Above this PST-400C TiO_2, smaller size TiO_2 (PST-30NRD) was coated with the same method mentioned above. The coating of PST-30NRD was repeated several times to create 18 μm thick TiO_2. The first layer of TiO_2 with 400 nm particle size served as a base layer to cover holes in FTS-MH. Without the first layer, the uniform coating was difficult to achieve and TiO_2 layers tended to crack after the annealing process due to weak contact between them. This layer also worked as a light scattering layer to enhance light absorption inside the photoanode. The second layer of TiO_2, 30 nm particle size, serves as the dye adsorption layer. Finally, FTS-MH coated with TiO_2 was immersed in the 0.3 mM solution of N719 dye in ethanol for 24 h at room temperature. Glass paper with a

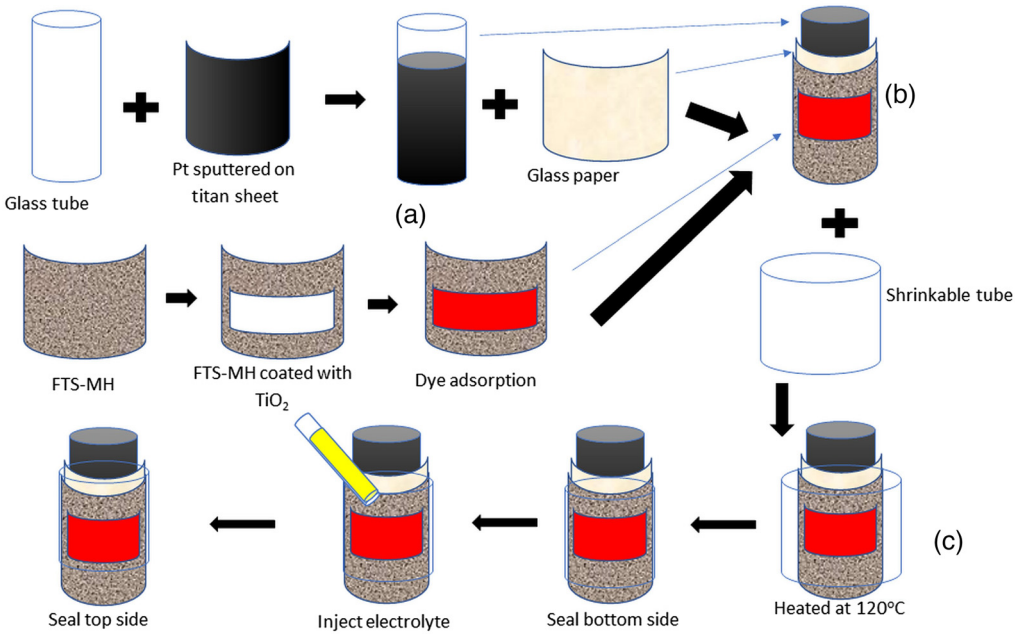

Fig. 1 Schematic representation of the device fabrication process for cylindrical TCO-free DSSC with FTS-MH as a working electrode. (a) Titanium foil/plastic spacer/cylinder glass. (b) Dye absorbed TiO_2-coated FTS-MH mesh 360 deg twisted. (c) All components inserted into a heat shrinkable-tube.

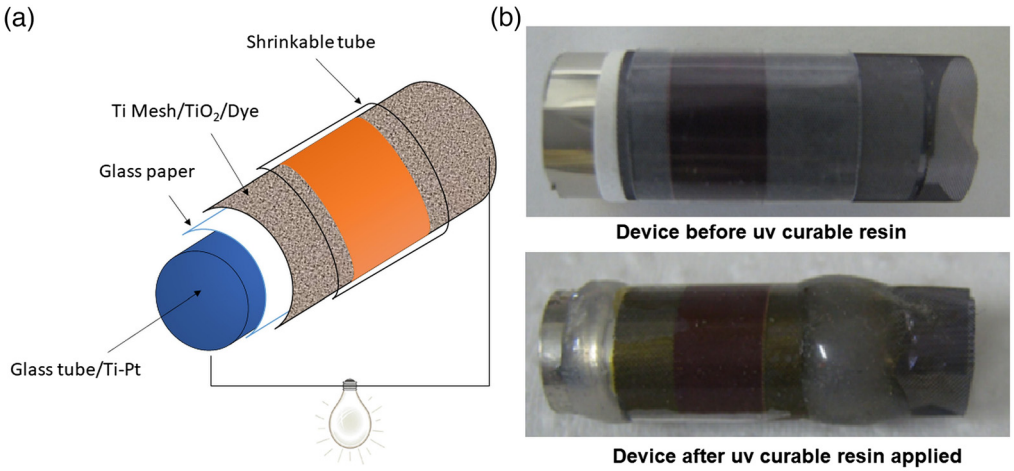

Fig. 2 (a) Fabricated cylindrical TCO-free DSSC schematics and (b) actual photographs.

thickness of 50 μm was wrapped over the Pt/Ti sheet/glass tube as a spacer in order to prevent short-circuiting and to hold the electrolyte. And then dye absorbed TiO_2-coated FTS-MH mesh was wrapped at the counter electrode, which was 360 deg twisted. [Fig. 1(b)]. After these all components were wrapped together, it was then inserted into a heat shrinkable-tube (NF070, FEP from JUNFLON Junkosha Inc. Japan) to heat at 120°C for 30 s [Fig. 1(c)]. The wall thickness of the tube after shrinking was 0.2 mm. This heat-shrinkable tube reduced the gap between photo anodes and counter electrodes to maintain the structure tight and compact (Fig. 2). The fabricated cylindrical structure was plastic tube/dye-TiO_2/FTS-MH/glass paper/Pt-Ti/glass tube (Fig. 2). One side of the cylinder was sealed with UV resin and solidified with UV light (Fig. 2). An electrolyte was inserted into the glass paper gap. The electrolyte composition was as follows: 0.05 M Iodine (I_2), 0.1 M lithium iodine (LiI), 0.5 M 4-tert-butylpyridine and 0.6 M 1,2-dimethyl-3 propylimidazolium iodine in acetonitrile. Finally, the other sides of the device were sealed with UV resin to prevent leakage and evaporation of the electrolyte. The silver paste was applied to both poles. The assembly process of the TCO-free cylindrical used in this work has been shown schematically in Fig. 1.

Photovoltaic performance of the DSSCs fabricated was measured by the Bunko-Keiki Co. Ltd. Model Solar Simulator (CEP-2000, Bunko Keiki, Japan). The illumination area during the photovoltaic measurement was controlled using black tape as a mask. The mask used for photovoltaic measurement of the cylindrical DSSC consisted of a black-colored insulating tape (180-μm thick) having an aperture area of 0.25 cm^2. It was attached to the outer wall of the cylindrical DSSC during the measurement. The mask was curved along with the surface of the cylinder. We used the mask with this aperture area (0.35 cm^2) for cylindrical TCO-free DSSCs in this work during solar cell performance evaluation as per our earlier report based on the laser beam-induced current (LBIC) measurement system.[22] In this measurement of LBIC profilometry of cylindrical solar cells, we have demonstrated that the distribution of induced current was highly uniform and constant in the area of the 6 mm $\times$ 10 mm for a cylindrical solar cell with a tube diameter of 4 to 5 mm. The light intensity was 100 mW/cm^2 used as the standard light for measuring PV performance (calibrated with Si solar cell). The photocurrent action spectra of the cylindrical solar cells were measured with a constant photon flux of 10^{16} photons per cm^2 at each wavelength in the DC mode. The incident photon-to-current conversion efficiency (IPCE) spectrum measurement system was connected to the CEP-2000 solar simulator.

3 Result and Discussion

Figure 3 shows the photocurrent density-voltage (J-V) characteristics of cylindrical TCO-free DSSCs with untreated FTS-MH and H_2O_2-treated FTS-MH with Pt-coated Ti-sheet as counter electrodes. It can be clearly seen from this figure that cylindrical DSSCs fabricated using

untreated FTS-MH exhibited much hampered PCE as compared to that utilizing FTH-MH treated with H_2O_2 as a photoanode/working electrode. After simulated solar irradiation of 100 mW/cm^2, DSSC with untreated FTS-MH showed a photoconversion efficiency (PCE), short-circuit current density (Jsc), open circuit voltage (Voc), and fill factor (FF) were 5.76%, 10.79 mA/cm^2, 0.74 V and 0.72, respectively. On the other hand, DSSCs utilizing a working electrode, where the FTS-MH surface was treated with H_2O_2 demonstrated a pronounced enhancement in the photovoltaic performance with PCE, Jsc, Voc, and FF of 8.59%, 16.19 mA/cm^2, 0.76 V, and 0.70, respectively. The larger pore size of glass paper used as a spacer and larger particle size (400 nm) of TiO_2 on FTS-MH acts as a support of electrolyte and dye adsorbed mesoporous TiO_2 layer allowing facile transport of redox species between the working and counter electrodes.[27] At the same time, this larger particle size promotes light trapping by scattering the incident photons on the photoanode. To explain this pronounced enhancement in Jsc of the cylindrical DSSCs using H_2O_2 treated FTS-MH working electrode, the photocurrent action spectrum after monochromatic light illumination was also recorded and is shown in Fig. 4. The IPCE as a function of wavelength of the incident light as shown in Fig. 4 clearly demonstrates that light absorption and photon harvesting in the whole photoactive region from 400 to 750 nm was enhanced for the cylindrical DSSC based on H_2O_2-treated FTS-MH photoelectrode as compared to that of DSSCs utilizing untreated FTS-MH photoelectrode counterparts. This enhanced photon harvesting is responsible for enhanced Jsc in the case of cylindrical TCO-less DSSCs utilizing H_2O_2-treated FTS-MH as a photoanode as shown in Fig. 3.

Such an enhanced PCE observed of cylindrical DSSCs using H_2O_2-treated FTS-MH as photoanode could be attributed to the improved charge collection and enhanced dye loading.[28] The TiO_2 nanosheet formed on the FTS-MH surface by H_2O_2 surface treatment provides a better interconnection between FTS-MH surface and coated mesoporous TiO_2 layer resulting in facile charge collection after the photon harvesting.[29,30] In our previous work, we have already shown that titanium nanosheets were formed by a chemical reaction between the Ti and hydrogen peroxide on the titanium surface making TiO_2 nanosheets leading to improved performance of the Ti-wire-based cylindrical TCO-free DSSCs.[27] The enhancement of Voc is explained by the formation of a charge recombination-blocking layer. Formed nanosheets on treated FTS-MH suppress the charge recombination of electrons in FTS-MH and I_3^- in the electrolyte. The calculated Jsc from IPCE is also shown in Fig. 4. FTS-MH photoelectrode-based cylindrical solar cells had 13 mA/cm^2 on the other hand untreated FTS-MH photoelectrode grid-based DSSC has 9 mA/cm^2. These calculated Jsc are in close agreement with observed Jsc from the J–V curve of Fig. 3. The distribution of photovoltaic parameters of fabricated cylinder solar cells are summarized in Fig. 5. To get more information about the reason behind higher Jsc on H_2O_2 treated

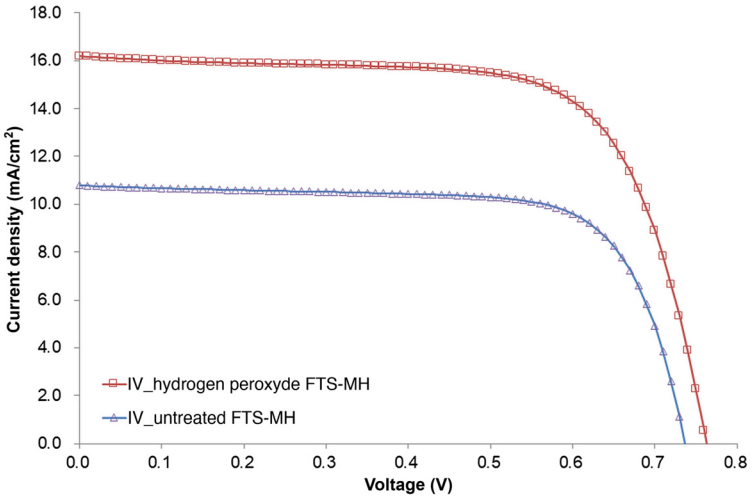

Fig. 3 Photovoltaic characteristics for the TCO-free cylindrical DSSCs using untreated and H_2O_2 treated FTS-MH for photoanode fabrication after simulated one sunlight irradiation.

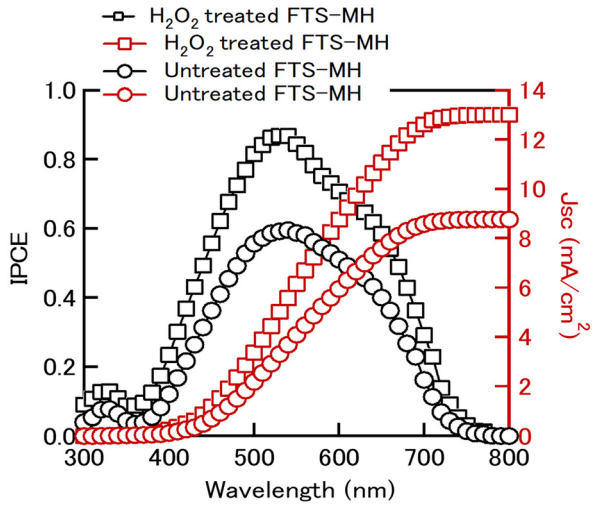

Fig. 4 Photocurrent action spectra for devices with and without H_2O_2 treatment on FTS-MH of cylinder TCO-free DSSCs after monochromatic light irradiation. The calculated Jsc from the integrated IPCE is shown on the right vertical axis.

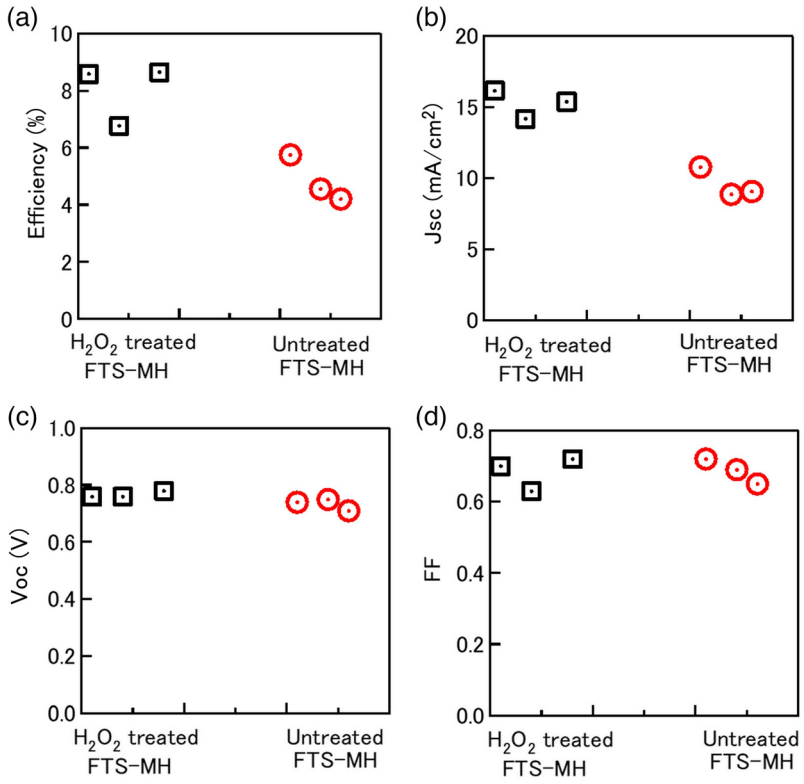

Fig. 5 Photovoltaic parameter distribution of three different cylindrical TCO-free DSSC fabricated in a batch. (a) PCE, (b) Jsc, (c) Voc, and (d) FF.

FTS-MH photoelectrode, dye loading was measured and calculated by comparing the desorption of N719 dyes with a calibration curve from a known concentration of dye and divided by the total area of the TiO_2 layer[31] as shown in Fig. 6. Dye solutions with the known concentrations were made and their absorption spectra were measured to make a calibration curve. To desorbed the dyes from the TiO_2 surface, using a mixture of NaOH (0.1 mM) in water, ethanol, t-butyl alcohol, and acetonitrile (1:1:1:1, v/v) was used. Using the calibration curve and results of the dye desorption studies, the amount of dye loading was calculated for H_2O_2-treated and untreated

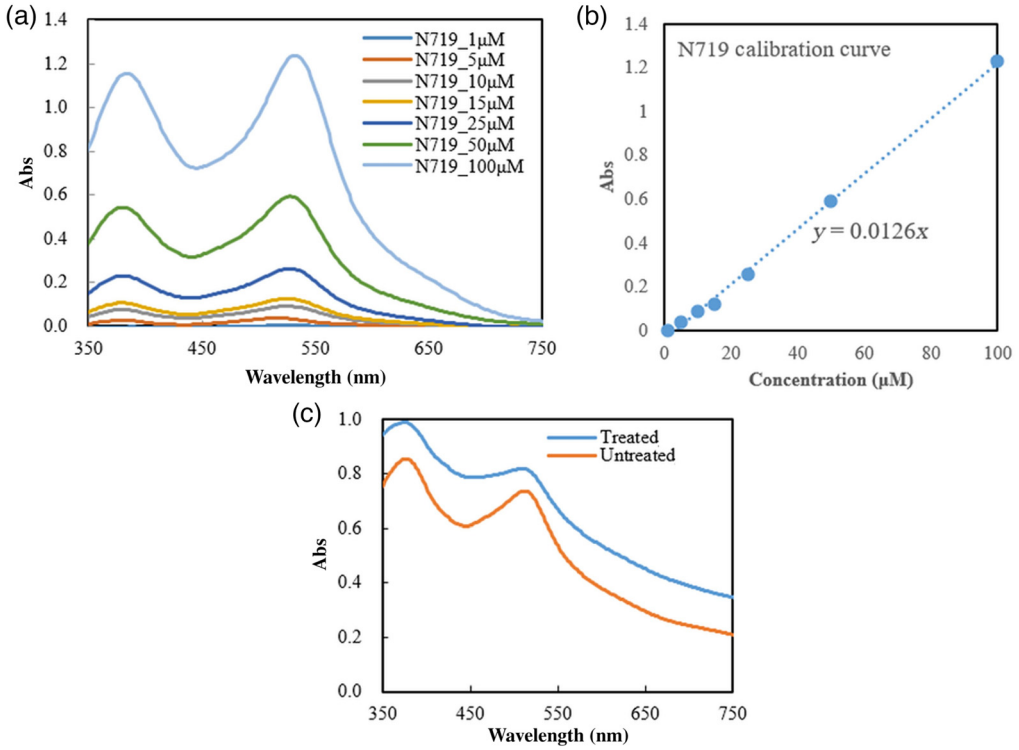

Fig. 6 (a) Absorption spectra for different concentrations of N719 dye (top left), (b) its calibration curve (top right), and (c) absorption spectra of desorbed dye from photoanodes for treated and untreated FTS-MH (bottom) used for dye loading estimation.

FTS-MH photoanodes. Treated FTS-MH has an absorption peak for the desorbed dye of 0.81, which corresponds to a concentration of 64.29 μM. Since the concentration was taken in 5 mL, the concentration of the dye desorbed was 321.45 nmole. The active area of titania is 1 cm^2 and gave the final dye loading for the H_2O_2 treated photoanode to be 321.45 nmole/cm^2. Using a similar experimental protocol, an absorption peak for the desorbed dye of 0.74, corresponds to the concentration of 58.73 μM giving a final dye loading of 293.65 nmole/cm^2 for untreated FTS-MH photoanode. Therefore, there was an 8.6% of enhancement in the dye loading upon the FTS-MH surface after the H_2O_2 surface treatment.

Therefore, the observed pronounced enhancement in Jsc in and PCE for devices using H_2O_2-treated FTS-MH photoanode as compared to its untreated photoanode device counterparts could be attributed to both of the enhanced dye loading facilitated by increased surface area due to anatase TiO_2 nanosheet formation and lower interfacial resistance between H_2O_2-treated FTS-MH substrate and mesoporous TiO_2 due to improved electrical contact between TiO_2 nanoparticles and the FTS-MH. Since dye loading was increased by only 8.6% and there was an enhancement of 33.3% and 32.9% in the Jsc and PCE, respectively, the second factor that the lower interfacial resistance facilitated by improved electrical contact can be considered as a dominant factor for the improvement in the device performance of cylindrical TCO-free DSSCs utilizing H_2O_2 treated FTS-MH photoelectrodes. The formation of dense anatase TiO_2 nanosheets improves electrical contact and facilitates charge transfer at the TiO_2/dye/electrolyte interface.[32,33] This improved electrical contact facilitates electron transfer from TiO_2 to FTS-MH, and a better TiO_2/dye/electrolyte interface with lower resistance facilitates electron injection, ultimately leading to increased Jsc.

4 Conclusion

Cylindrical TCO-free DSSCs utilizing FTS-MH as a substrate have been successfully fabricated and characterized. Treatment of FTS-MH substrate with H_2O_2 led to pronounced enhancement in the photovoltaic performance especially the Jsc of devices, which was attributed to the

formation of nanosheet of anatase TiO_2. Formation of this TiO_2 nanosheet on the FTS-MH surface by H_2O_2 treatment not only improved the dye-loading but also lowers interfacial resistance facilitating improved electrical contact between the conducting substrate surface and dye adsorbed mesoporous TiO_2 layer leading to retardation in charge recombination and improvement in the charge collection. The improvement in PCE from 5.76% to 8.59% (32.9%) after the H_2O_2 treatment could be attributed mainly due to the lower interfacial resistance facilitated by improved electrical contact since enhancement in the dye loading was only 8.6%. To the best of our knowledge, the PCE being reported is the highest value reported for TCO-free DSSCs with cylindrical structures.

References

1. F. W. Low and C. W. Lai, "Recent developments of graphene-TiO_2 composite nanomaterials as efficient photoelectrodes in dye-sensitized solar cells: a review," *Renew. Sustain. Energy Rev.* **82**, 103–125 (2018).
2. A. Omar, M. S. Ali, and N. Abd Rahim, "Electron transport properties analysis of titanium dioxide dye-sensitized solar cells (TiO_2-DSSCs) based natural dyes using electrochemical impedance spectroscopy concept: a review," *Sol. Energy* **207**, 1088–1121 (2020).
3. J. E. Boercker, E. Enache-Pommer, and E. S. Aydil, "Growth mechanism of titanium dioxide nanowires for dye-sensitized solar cells," *Nanotechnology* **19**(9), 095604 (2008).
4. S. N. F. Zainudin, H. Abdullah, and M. Markom, "Electrochemical studies of tin oxide based-dye-sensitized solar cells (DSSC): a review," *J. Mater. Sci.: Mater. Electron.* **30**(6), 5342–5356 (2019).
5. Q. Wali, A. Fakharuddin, and R. Jose, "Tin oxide as a photoanode for dye-sensitised solar cells: current progress and future challenges," *J. Power Sources* **293**, 1039–1052 (2015).
6. R. Vittal and K. C. Ho, "Zinc oxide based dye-sensitized solar cells: a review," *Renewable Sustainable Energy Rev.* **70**, 920–935 (2017).
7. T. Prakash, "Review on nanostructured semiconductors for dye sensitized solar cells," *Electron. Mater. Lett.* **8**(3), 231–243 (2012).
8. J. Gong et al., "Review on dye-sensitized solar cells (DSSCs): advanced techniques and research trends," *Renew. Sustain. Energy Rev.* **68**, 234–246 (2017).
9. S. Hwang et al., "Dye-sensitized solar cell counter electrodes based on carbon nanotubes," *ChemPhysChem* **16**(1), 53–65 (2015).
10. H. Wang and Y. H. Hu, "Graphene as a counter electrode material for dye-sensitized solar cells," *Energy Environ. Sci.* **5**(8), 8182–8188 (2012).
11. M. Zalas and K. Jelak, "Optimization of platinum precursor concentration for new, fast and simple fabrication method of counter electrode for DSSC application," *Optik* **206**, 164314 (2020).
12. M. M. Raikwar et al., "Biphenyl-amine-based D-π-A'-π-A sensitizers for DSSCs: comparative photo-conversion efficiency in iodide/triiodide and cobalt-based redox electrolyte and DFT study," *ChemistrySelect* **4**(24), 7371–7379 (2019).
13. S. Balamurugan and S. Ganesan, "Novel cobalt redox materials admitted in natrosol polymer with a thiophene based additive as a gel polymer electrolyte to tune up the efficiency of dye sensitized solar cells," *Electrochim. Acta* **329**, 135169 (2020).
14. C. L. Melissa, "Solyndra—illuminating energy funding flaws?" *Scientific American* (2011).
15. M. Bathon, "Solyndra lenders ahead of government won't recover fully," *Bloomberg Business* (2011). Retrieved 23 March 2022.
16. R. D. White, "Solar panel firm Solyndra to cease operations," *Los Angeles Times* (2011). Retrieved 23 March 2022.
17. J. Kalowekamo and E. Baker, "Estimating the manufacturing cost of purely organic solar cells," *Sol. Energy* **83**(8), 1224–1231, (2009).
18. S. Rahman et al., "Design & implementation of a dual axis solar tracking system," *Am. Acad. Scholarly Res. J.* **5**(1), 47–54 (2013).
19. Z. Tachan, S. Rühle, and A. Zaban, "Dye-sensitized solar tubes: a new solar cell design for efficient current collection and improved cell sealing," *Sol. Energy Mater. Sol. Cells* **94**(2), 317–322 (2010).

20. A. K. Baranwal et al., "Combining novel device architecture and NIR dye towards the fabrication of transparent conductive oxide-less tandem dye sensitized solar cells," *Appl. Phys. Express* **8**(10), 102301 (2015).
21. A. K. Baranwal et al., "Tandem dye-sensitized solar cells based on TCO-less back contact bottom electrodes," *J. Phys.: Conf. Ser.* **704**(1), 012003 (2016).
22. J. Usagawa et al., "Transparent conductive oxide-less three-dimensional cylindrical dye-sensitized solar cell fabricated with flexible metal mesh electrode," *Prog. Photovoltaics: Res. Appl.* **21**(4), 517–524 (2013).
23. A. K. Baranwal et al., "Tandem dye-sensitized solar cells with a back-contact bottom electrode without a transparent conductive oxide layer," *RSC Adv.* **4**(88), 47735–47742 (2014).
24. J. Usagawa et al., "Flexible transparent conductive oxide-less flat and cylinder dye-sensitized solar cells," *J. Photonics Energy* **2**(1), 021011 (2012).
25. G. Kapil et al., "Fabrication and characterization of coil type transparent conductive oxide-less cylindrical dye-sensitized solar cells," *RSC Adv.* **4**(44), 22959–22963 (2014).
26. S. G. Steinemann, "Titanium—the material of choice?" *Periodontology 2000*, **17**(1), 7–21 (1998).
27. A. Hayat et al., "Transparent conductive oxide-less back contact dye-sensitized solar cells using flat titanium sheet with microholes for photoanode fabrication," *J. Photonics Energy* **7**(1), 015501 (2017).
28. G. Kapil et al., "Titanium wire engineering and its effect on the performance of coil type cylindrical dye sensitized solar cells," *Org. Electron.* **15**(11), 3399–3405 (2014).
29. S. Tang et al., "Harnessing hierarchical architectures to trap light for efficient photoelectrochemical cells," *Energy Environ. Sci.* **13**(3), 660–684 (2020).
30. T. Y. Tsai et al., "An efficient titanium-based photoanode for dye-sensitized solar cell under back-side illumination," *Progr. Photovoltaics Res. Appl.* **21**(2), 226–231 (2013).
31. M. Hočevar et al., "One step preparation of TiO_2 layer for high efficiency dye-sensitized solar cell," *Acta chim. sloven.* **57**(2), 405–409 (2010).
32. C. H. Lee et al., "Improved performance of flexible dye-sensitized solar cells by introducing an interfacial layer on Ti substrates," *J. Mater. Chem.* **21**(13), 5114–5119 (2011).
33. H. G. Yun et al., "Effect of increased surface area of stainless steel substrates on the efficiency of dye-sensitized solar cells," *Appl. Phys. Lett.* **93**(13), 133311 (2008).

Biographies of the authors are not available.